Coherent Detection With Double-Side Vertically Illuminated Photodiodes for Spatially Resolved Ranging Applications

Pascal Rustige, Felix Ganzer, Patrick Runge, and Martin Schell

***Abstract*—We theoretically investigate and demonstrate coherent detection with double-side vertically illuminated photodiodes by injecting signal and local oscillator (LO) collinearly from opposite sides of the photodetector chip. This avoids optical combiners in front of the detector surface resulting in a 4.5 dB advantage over conventional coherent detection with 50-50 beam splitters to combine signal and LO. The heterodyne efficiency in the case of counter-propagating signal and LO exhibits a penalty of 1.5 dB at optimal absorption layer thickness compared to co-propagating signal and LO and has the same pronounced dependency on the relative propagation angle. A first proof of concept for using this dependency for spatially resolved coherent lidar systems is demonstrated.**

***Index Terms*—Coherent detection, double-side illumination, photodetector, ranging, lidar.**

I. Introduction

COHERENT light detection and ranging, like frequency-modulated-continuous-wave (FMCW)-lidar, is considered to have several advantages over direct detection approaches, like pulsed time-of-flight lidar [1]. FMCW-lidar extracts the range information by mixing the LO with the back reflection of the send out signal inside a photodetector. The generated radio frequency (RF) signal is dependent on both the signal power and the LO power. Hence tuning the latter provides adjustable gain and enables the retrieval of very low power backscattered signals. FMCW-lidar systems are considered insensitive to background noise due to, e.g., solar glare, or other lidar systems [2]. They also provide the velocity information due to the detectable Doppler frequency shift [3]. As coherent detection is widely applied in optical fiber and free-space communication, transferring coherent lidar systems to photonic integrated circuits (PICs) is a promising approach for the reduction of footprint and costs [4].

However, apart from the development of low noise and narrow linewidth tunable lasers [5], fast beam steering and efficient free space to fiber/chip coupling are major challenges for PICs targeting the generation of a full 3D data point cloud of the environment [1]. Lidar-systems based on focal plane arrays (FPA), where receiver pixels are positioned at the focal plane of a lens, circumvent the requirement of beam steering, but are mainly restricted to direct time-of-flight solutions. Rogers *et al.* demonstrated a coherent FPA 3D imaging sensor on a silicon photonics platform, but were challenged by matching the receiver and the transmitter focal plane in combination with the optical lens system [1]. Other FPA-based coherent receivers use 50-50 optical beam splitters to combine signal and LO and therefore require accurate collinear superimposition of signal and LO and suffer from a fourfold reduction in signal strength [6], [1]. In [7], we proposed a novel approach of spatially resolved coherent detection by illuminating the photodetector chips with signal and LO from opposite sides for coherent detection. This has the potential for array configurations with coherent detection in a single photodetector.

In this article, we compare heterodyne coherent detection with counter-propagating signal and LO to the co-propagating case with using 50-50 beam splitters. We experimentally confirm the in [7] proposed approach superseding optical beam splitters and delivering new degrees of freedom in the design of solid-state coherent lidar systems by making use of the strong intermediate frequency (IF) power dependency on the relative propagation angle between signal and LO.

II. RF Generation via Double-Sided Photodiode Illumination

A. Theory of RF Generation via Optical Field Mixing

The electrical field components of the signal light and LO light mixed in a photodetector can be written in the form

$$\begin{aligned}\vec{E}_{\mathrm{S}}(\vec{r},\mathrm{t}) &= \vec{A}_{\mathrm{S}}(\vec{r})\cos\left(2\pi\nu_{\mathrm{S}}t+\phi_{\mathrm{S}}\right),\\ \vec{E}_{\mathrm{LO}}(\vec{r},\mathrm{t}) &= \vec{A}_{\mathrm{LO}}(\vec{r})\cos\left(2\pi\nu_{\mathrm{LO}}t+\phi_{\mathrm{LO}}\right),\end{aligned} \tag{1}$$

where $\vec{A}_{\mathrm{S}}(\vec{r})$ and $\vec{A}_{\mathrm{LO}}(\vec{r})$ are the amplitudes, ν_{S} and ν_{LO} are the optical frequencies, and ϕ_{S} and ϕ_{LO} are the phase of signal and LO. On square-law photodetectors the total incident power P is proportional to the integral over the aperture area A of the square of the combined electric fields $\vec{E}_{\mathrm{S}}$ and $\vec{E}_{\mathrm{LO}}$:

$$P \sim \int_A \left|\vec{E}_{\mathrm{S}}+\vec{E}_{\mathrm{LO}}\right|^2 \mathrm{d}^2 r, \tag{2}$$

Manuscript received December 1, 2021; revised February 2, 2022; accepted February 24, 2022. Date of publication March 7, 2022; date of current version March 16, 2022. This work was supported by the Fraunhofer Society under the PREPARE project MELINDA. *(Corresponding author: Pascal Rustige.)*

The authors are with the Fraunhofer-Institut für Nachrichtentechnik Heinrich-Hertz-Institut HHI, 10587 Berlin, Germany (e-mail: pascal.rustige@hhi.fraunhofer.de; felix.ganzer@hhi.fraunhofer.de; patrick.runge@hhi.fraunhofer.de; martin.schell@hhi.fraunhofer.de).

Color versions of one or more figures in this article are available at https://doi.org/10.1109/JSTQE.2022.3156641.

Digital Object Identifier 10.1109/JSTQE.2022.3156641

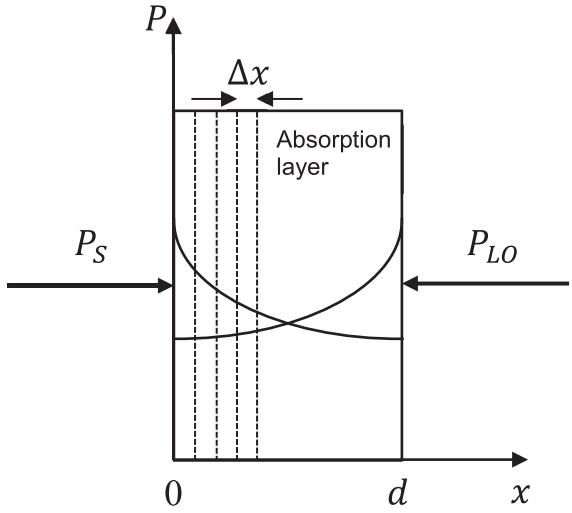

Fig. 1. Cross section of a coherent photodetector, visualizing the power overlap inside the absorption layer of thickness d for the case of counter-propagating signal and LO.

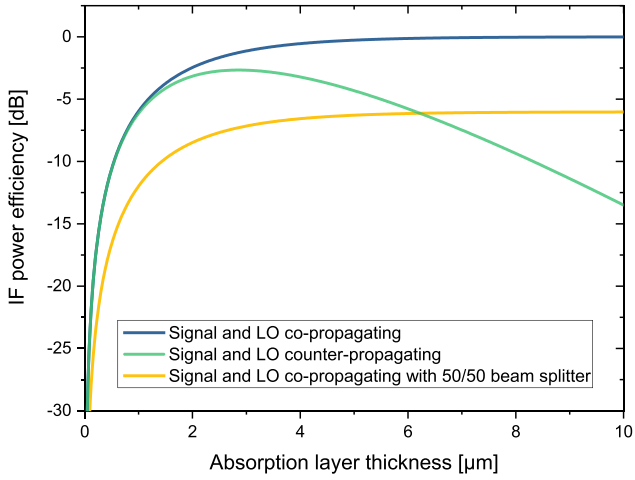

Fig. 2. IF power efficiencies as functions of the absorption layer thickness of a photodiode in cases of co-propagating signal and LO with and without, as well as counter-propagating signal and LO for an InGaAs absorption layer with $\alpha = 0.7/\mu m$ and an optical wavelength of 1.55 μm.

therefore creating an intermediate frequency $f_{\mathrm{IF}} = |\nu_{\mathrm{S}} - \nu_{\mathrm{LO}}|$ and sum frequency part. Neglecting the latter, with its frequency normally beyond the detector bandwidth, this leads to a total photocurrent of

$$i_{\mathrm{tot}}\ (t)\ = i_{\mathrm{DC}}\ + i_{\mathrm{IF}} \cos\left(2\pi f_{\mathrm{IF}} t + \Delta\phi\right), \tag{3}$$

$$i_{\mathrm{DC}} = \frac{e}{h\nu}\ \eta\ \left(\varepsilon P_{\mathrm{S}} + (1-\varepsilon)\, P_{\mathrm{LO}}\right), \tag{4}$$

$$i_{\mathrm{IF}} = \frac{2e}{h\nu}\ \eta\ \sqrt{(\varepsilon - \varepsilon^2)\, P_{\mathrm{S}} P_{\mathrm{LO}}}, \tag{5}$$

for optically combined signal and LO, where η is the detector quantum efficiency, e the elementary electric charge, h the Planck constant, $\Delta\phi$ the optical phase offset, P_{S} the optical signal power, P_{LO} the local oscillator optical power and ε the splitting ratio of the optical beam splitter, if assuming same polarization of signal and LO. Tuning P_{LO} creates adjustable amplification of the IF part, in theory up to the shot noise limit. Equations (3)–(5) only hold up for signal and LO co-propagating under the same angle of incidence, being conventionally realized with beam splitters acting as optical combiners. The optimum splitting ratio ε is evidently 0.5 , resulting in a 6 dB loss of the electrical RF power, being proportional to the square of i_{IF}.

B. Counter-Propagating Signal and Local Oscillator

In the counter-propagating case, signal and LO penetrate the absorption layer of the photodiode from opposite sides. This means that the light of signal and LO will have a reduced overlap resulting in a reduction of heterodyne efficiency. For solving the overlap integral, one has to take the exponential decay of the optical power into account (Beer-Lambert law):

$$P\ (x) = P_0\ \cdot e^{-\alpha x}, \tag{6}$$

where $P(x)$ is the power at penetration depth x and α is the wavelength and material dependent absorption coefficient. For the co-propagating case, this is implicitly included in the definition of the photodiode's quantum efficiency

$$\eta\ =\ 1 - e^{-ad}, \tag{7}$$

where d is the total thickness of the absorption layer of the photodetector.

Fig. 1 visualizes the reduction of optical power P inside the absorption layer for the counter-propagating case. A reduction of IF power is to be expected, due to the reduced overlap of signal and LO inside the detector. The IF current for the counter-propagating case is obtained by solving the integral

$$i_{\mathrm{IF}} = \frac{2e}{h\nu}\ \cdot \int_0^d \sqrt{\beta P_S\,(x) \cdot \beta P_{LO}\,(x)}\mathrm{d}x \tag{8}$$

over the absorption layer thickness d, where $\beta \cdot \Delta x$ is the fraction of power absorbed by the infinitesimal absorption distance $\Delta x \to 0$:

$$\beta\ =\ \lim_{\Delta x \to 0}\left[\frac{1 - e^{-\alpha \Delta x}}{\Delta x}\right]\ =\ \alpha. \tag{9}$$

With

$$\begin{aligned} P_S\,(x)\ &= P_S\ e^{-\alpha x}\,, \\ P_{LO}\,(x)\ &= P_{LO}\ \ e^{\alpha(x-d)} \end{aligned} \tag{10}$$

we obtain the result

$$\begin{aligned} P_{IF}\ &\sim\ \left[\int_0^d \sqrt{\alpha P_S e^{-\alpha x} \cdot \alpha P_{LO} e^{\alpha(x-d)}}dx\right]^2 \\ &= P_{\mathrm{S}}\ P_{\mathrm{LO}} \cdot \alpha^2 d^2\ e^{-\alpha d} \end{aligned} \tag{11}$$

providing a correction factor for the IF power. Small values of d correspond to the conventional co-propagating case. As expected, for large values of d the efficiency approaches zero. The overlap and hence the generated IF power is maximum at $d\ =\ 2/\alpha$, and the maximum becomes material and wavelength independent with a value of $4/e^2$.

Fig. 2 shows the IF power efficiencies as functions of the absorption layer thickness d for counter-propagating signal and LO in comparison to same side illumination with and without use of a 50-50 beam splitter for the exemplary case of 1.55 µm wavelength and an InGaAs absorption layer with an absorption coefficient of 0.7/µm at this wavelength [8]. The maximum generated IF power for the counter-propagating light is around 3 µm absorption layer thickness, being a typical value for highly efficient InGaAs photodiodes. At this value, the relative IF power at zero relative propagation angle between signal and LO compared to the co-propagating case is only -1.5 dB, while it is 4.5 dB compared to the 50-50 splitter case.

The proposed concept of counter-propagating signal and LO is evidently not constrained to InGaAs-based photodiodes, but can be transferred to any photodiodes suitable for illumination from both sides. Therefore, coherent detection at different wavelengths, e.g., with silicon(-germanium) PIN photodiodes is possible, as long as the thickness of the absorption layer and its absorption coefficient allow for a substantial overlap of the optical fields of signal and LO, see Eq. (11).

III. Proof of Concept

A. Experimental Setup

Fig. 4 shows the experimental setup for a proof of concept. The setup allows for determining the relative propagation angle dependency of the IF signal power generated through counter-propagating signal and LO, optically mixed inside an InGaAs photodiode chip. The two laser inputs opposite of each other were tuned to a wavelength offset of $\Delta\lambda = (15 \pm 5)$ pm, corresponding to an IF frequency of $f_{\mathrm{IF}} \approx (0.5 \pm 0.1)$ GHz at $\lambda = 1.55\ \mu$m. One laser input was tunable in its angle of incident in the range of $\pm 6°$. An additional input can illuminate the photodiode in an angle of incident of about 50°. The polarization of the front side inputs can be matched to the backside input by means of polarization controllers.

The IF output power level was measured with a broadband RF power meter and recorded with a spectrum analyzer. Fig. 5 shows the electrical RF power spectrum with a distinct signal at the expected frequency, vanishing after deactivation of either of the two inputs.

B. Influence of Relative Angle of Signal and Local Oscillator

In the co-propagation case, the heterodyne efficiency is highly dependent on the relative propagation angle of signal and LO. The loss factor due to misalignment of signal and LO shows a Bessel function like dependency on the relative propagation angle $\Delta\theta$, while the relative polarization mismatch $\Delta\psi$ reduces the IF power proportional to its cosine [9]. The overall loss function is

$$L\ (\Delta\psi, \Delta\theta,\ D) = \cos\Delta\psi\ \cdot \left| \frac{2J_1\ (\pi\Delta\theta D/\lambda)}{\pi\Delta\theta D/\lambda} \right|, \qquad (12)$$

where J_1 is the first order Bessel function of the first kind and D the optical aperture. Fig. 3 shows the normalized IF signal power against the relative propagation angle $\Delta\theta$ measured for two different apertures at an optical wavelength of $\lambda = 1.55\ \mu$m

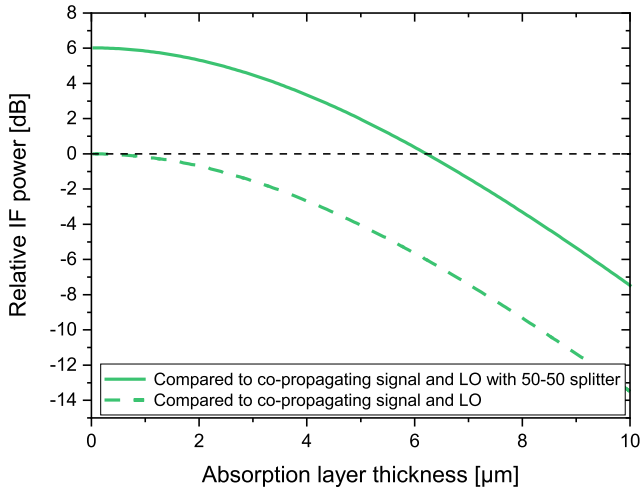

Fig. 3. Resulting relative IF power as a function of the absorption layer thickness of a coherent detector in case of signal and LO counter-propagating in an InGaAs absorption layer at 1.55 µm optical wavelength.

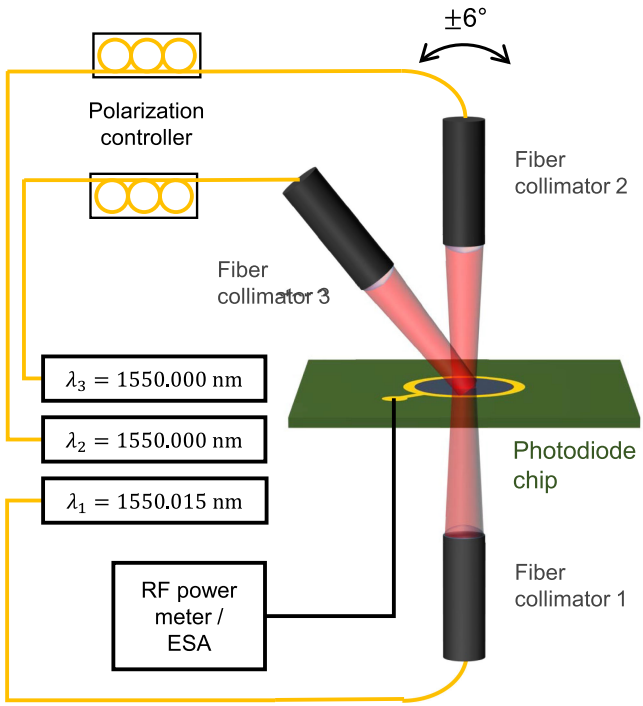

Fig. 4. Measurement setup for experimental demonstration of the novel concept.

for counter-propagating signal and LO. For the 109 µm aperture, the IF power drops to less than 15% at angle offsets bigger than only one degree. Fits with Eq. (12) coincide well with the measurement data, which gives evidence that in the case of counter-propagating signal and LO, the heterodyne efficiency exhibits the same dependency on the relative propagation angle as in the co-propagating case. In case of the 39 µm aperture size the measured values for angles >3° do not reach the expected power levels due to the decrease of the effective cross-section of laser beam and photodiode.

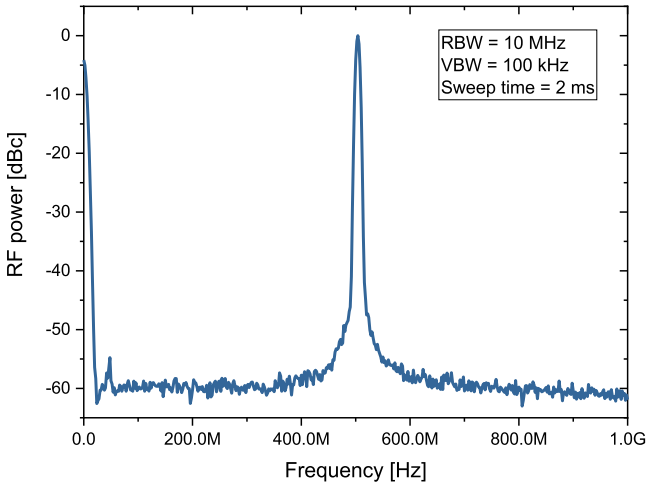

Fig. 5. RF power spectrum of the intermediate frequency signal generated via heterodyne optical mixing of two continuous wave laser at a wavelength of 1,55 µm illuminated from opposite sides of an InGaAs photodetector chip.

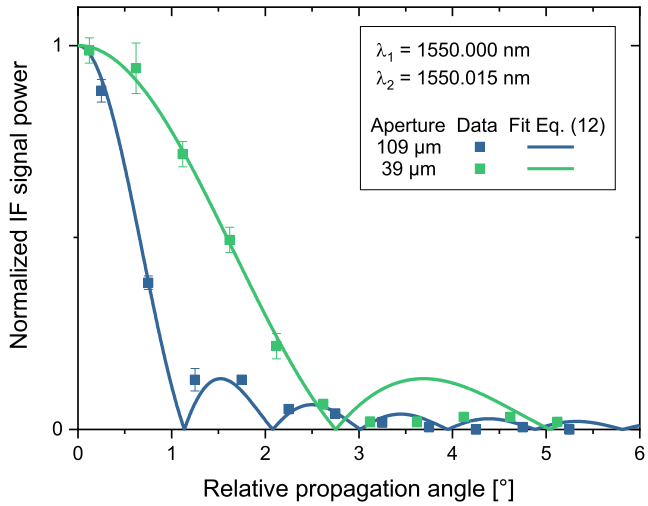

Fig. 6. Loss factor of the heterodyne efficiency as a function of the relative propagation angle of counter-propagating signal and LO for different aperture sizes and an optical wavelength of 1.55 µm.

IV. Spatially Resolved Coherent Detection Due to Double-Sided Illumination

Compared to direct time-of-flight lidar based on FPAs, one of the main challenges for coherent lidar is the spatial resolution of the environment. This section shall provide two approaches to overcome this drawback for coherent detection.

The significant IF power drop under non-collinear angles of propagation of signal and LO constitutes a nuisance in free-space optical coherent detection [10], as signal and LO have to be carefully matched to guarantee efficient IF generation. In [7] we suggested the new concept of using the strong angle dependency as a key feature for deliberate suppression of signals under all angles of no interest. Sweeping the relative angle between signal and LO or using suitable lens and array combinations, one is able to create a spatially resolved coherent detection with angle

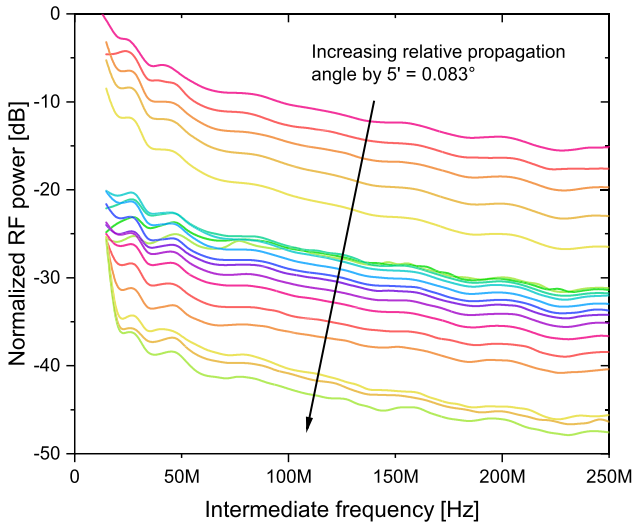

Fig. 7. RF power spectrum of an InGaAs photodiode with aperture size of 1 mm illuminated with light of 1.55 µm wavelength by fiber collimators of 0.20 mm spot size. For increasing relative propagation angle of signal and LO the measured RF power decreases periodically.

resolution. The implementation of an angle sweep in coherent receiver systems with optical beam splitters is challenging due to the requirement of matching signal and LO on the detector surface under all angles. Injecting the LO light from the other side of the photodetector chip, however, circumvents this obstacle and creates the essential feature of only generating IF power for the collinear signal impinging on the detector. For an exemplary aperture of 1 mm, a photodiode size still providing sufficient bandwidth, while ensuring capturing as much backscattered light as possible, Eq. (12) predicts an 8.8 dB reduced first side-lobe at 0.15°, corresponding to 13% IF power.

Fig. 7 shows the measured IF power spectrum of a 1 mm photodiode illuminated with signal and LO counter-propagating for increasing relative propagation angles. The wavelengths of our used lasers are drifting relative to each other in time, corresponding to an IF fluctuation in the range of few hundred MHz. As the RF power output of the investigated 1 mm photodiode chip shows a non-negligible RC-bandwidth decay in this frequency regime, we intentionally swept the relative wavelength of the signal and the LO and acquired the RF power spectrum up to 250 MHz with an electrical spectrum analyzer by using the *max hold* functionality. The relative IF power can be extracted for a constant IF. The IF instability does not occur in a real FMCW-lidar system, as signal and LO originate from the same laser source.

Fig. 8 shows the relative IF signal power for increasing relative propagation angle extracted from Fig. 7. The measured data does not comply with the expected power drop of the IF signal for a 1 mm aperture, but the positions of minima and maxima coincide with a theoretical 0.20 mm aperture. This value corresponds to the biggest spot size of the used fiber collimators that were available to us.

However, we successfully were able to demonstrate IF signal generation by mixing counter-propagating signal and LO inside

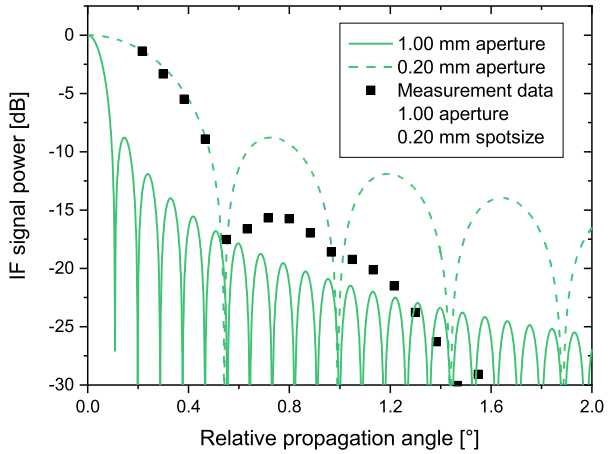

Fig. 8. IF signal decay as a function of the relative propagation angle of signal and LO in coherent detection for an aperture size of 1 mm and 0.2 mm at an optical wavelength of 1.55 µm. Measurement data extracted from Fig. 7 for 1 mm aperture and 0.2 mm spot size.

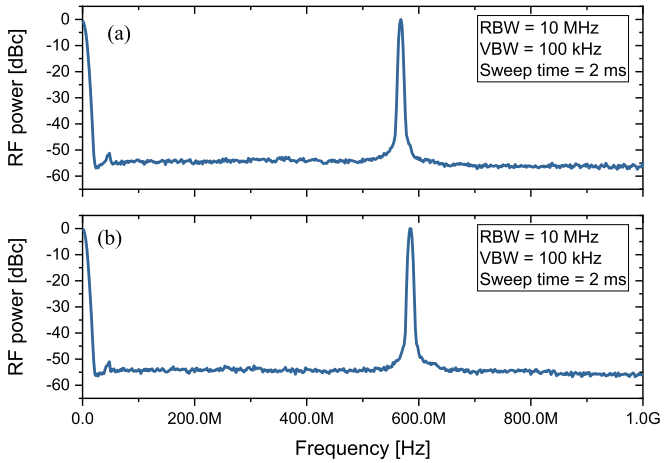

Fig. 9. RF power spectrum of the intermediate frequency signal generated via heterodyne optical mixing of (a) two continuous wave laser at a wavelength of 1,55 µm illuminated from opposite sides of an InGaAs photodetector chip and (b) with an additional third laser input under a flat angle. The slight shift towards higher frequencies is an effect of using two independent lasers.

a large-aperture photodiode that theoretically could make angle resolutions in the order of 0.1 feasible, if deployed in coherent lidar systems by sweeping the relative angle of signal and LO.

To prove this characteristic further, we installed a third fiber collimator in our setup (see Fig. 4) and coupled additional optical power of same wavelength under a flatter angle of ∼50° into the photodiode chip.

While the DC current i_{DC} increased according to the responsivity of the photodiode, no increase of RF power or no additional signal in the spectrum was observable, see Fig. 9. The slight shift in frequency is due to the aforementioned wavelength difference drift of the two lasers at times of acquisition.

Based on this proof of concept, the two following approaches for spatially resolved coherent detection are proposed, both providing new approaches for developing solid-state coherent receivers for ranging applications.

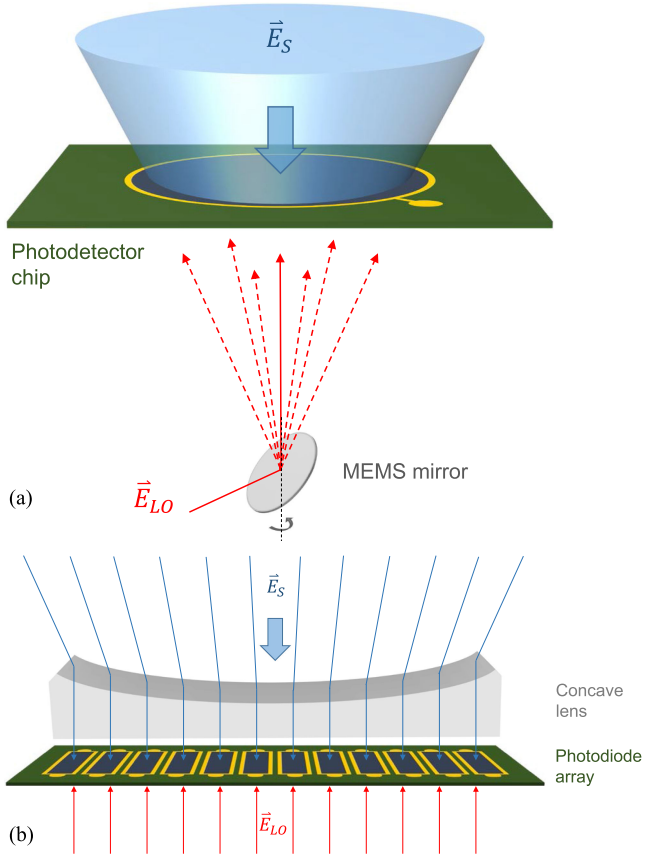

Fig. 10. Concept for spatially resolved coherent detection with illumination of signal and LO from opposite sides of the photodetector chip by (a) sweeping the angle of LO by means of a, e.g., MEMS mirror and (b) separating different angular signal parts of the field-of-view and matching with the LO on different array elements of the detector.

Using compact LO beam steering, e.g., by MEMS mirrors, in close proximity of the photodiode chip backside, would make the proposed angle sweep feasible. Fig. 10a) illustrates a potential realization of a receiver configuration by positioning a photodiode with large aperture in front of the focal plane and an LO sweep at focus. Only angular parts of the signal that are collinear with the momentary angle of the LO will contribute to the IF signal power, and thereby provide a way to scan through the field-of-view of the photodetector aperture.

An alternative concept avoiding moving parts is shown in Fig. 10b), where individual array elements receive signal power from different parts of the field-of-view via the lens system in front of a receiver array. If a uniform, homogenous backside illumination of the array can be provided, this approach represents a scalable concept for coherent detection with non-moving elements, and can potentially be extended to 2D configurations by use of electrodes based on transparent conducting material, e.g., indium tin oxide (ITO).

V. Conclusion

We demonstrated a proof of concept for coherent detection with double-side vertically illuminated photodiodes for spatially

resolved ranging applications, where signal and LO are injected collinearly from opposite sides of the photodiode chip. We conclude that the fourfold reduction of the signal strength in the case of using optical beam splitters for same-side illumination can be mitigated and even improves the performance. The possibility of sweeping the relative angle between the receiving signal and the LO provides new concepts of scalable and compact spatially resolving coherent detectors for sensing and ranging applications. The use of photodiodes with about 1 mm aperture could allow for angle resolutions in the order of 0.1°.

REFERENCES

[1] C. Rogers *et al.*, "A universal 3D imaging sensor on a silicon photonics platform," *Nature*, vol. 590, no. 7845, Feb. 2021, Art. no. 7845, doi: 10.1038/s41586-021-03259-y.

[2] B. Behroozpour, P. A. M. Sandborn, M. C. Wu, and B. E. Boser, "Lidar system architectures and circuits," *IEEE Commun. Mag.*, vol. 55, no. 10, pp. 135–142, Oct. 2017, doi: 10.1109/MCOM.2017.1700030.

[3] H. D. Griffiths, "New ideas in FM radar," *Electron. Commun. Eng. J.*, vol. 2, no. 5, pp. 185–194, 1990.

[4] B. J. Isaac, B. Song, S. Pinna, L. A. Coldren, and J. Klamkin, "Indium phosphide photonic integrated circuit transceiver for FMCW LiDAR," *IEEE J. Sel. Topics Quantum Electron.*, vol. 25, no. 6, Nov. 2019, Art. no. 8000107, doi: 10.1109/JSTQE.2019.2911420.

[5] A. Martin *et al.*, "Photonic integrated circuit based FMCW coherent LiDAR," *J. Lightw. Technol.*, vol. 36, no. 19, pp. 4640–4645, Oct. 2018, doi: 10.1109/JLT.2018.2840223.

[6] M. L. Simpson *et al.*, "Coherent imaging with two-dimensional focal-plane arrays: Design and applications," *Appl. Opt.*, vol. 36, no. 27, pp. 6913–6920, Sep. 1997, doi: 10.1364/AO.36.006913.

[7] P. Rustige, P. Runge, F. M. Soares, J. Krause, and M. Schell, "A new concept for spatially resolved coherent detection with vertically illuminated photodetectors targeting ranging applications," in *Proc. Opt. Compon. Mater. XVIII*, 2021, pp. 18–24. doi: 10.1117/12.2576323.

[8] F. R. Bacher, J. S. Blakemore, J. T. Ebner, and J. R. Arthur, "Optical-absorption coefficient of ingaas/InP," *Phys. Rev. B*, vol. 37, no. 5, pp. 2551–2557, Feb. 1988, doi: 10.1103/PhysRevB.37.2551.

[9] C. C. Chen and C. S. Gardner, "Comparison of direction and heterodyne detection optical intersatellite communication links," Electro-Optic Syst. Lab., Dept. Elect. Comput. Eng., College Eng., Univ. Illinois, Urbana, Illinois, Tech. Rep. EOSL NO. 87-002, 1987.

[10] Y. Ren, A. Dang, L. Liu, and H. Guo, "Heterodyne efficiency of a coherent free-space optical communication model through atmospheric turbulence," *Appl. Opt.*, vol. 51, no. 30, pp. 7246–7254, Oct. 2012, doi: 10.1364/AO.51.007246.

Pascal Rustige received the M.Sc. degree in physics from the Humboldt University of Berlin, Berlin, Germany, in 2017. Since then, he has been with the Fraunhofer Heinrich Hertz Institute as a Research Associate. His research interests include InP-based photonic detectors for sensing and quantum communication. He is a Member of Optica and SPIE.

Felix Ganzer, photograph and biography not available at the time of publication.

Patrick Runge received the Dipl.-Ing. degree in computer science and the Ph.D. degree in electrical engineering from the Technical University of Berlin, Berlin, Germany, in 2005 and 2010, respectively. From 2005 to 2007, he was with the Hymite GmbH, where he was involved in the RF design and measurement of optoelectronic packages for optical communication. In 2007, he returned to the Technical University of Berlin to pursue the Ph.D. degree, where he investigated nonlinear effects and applications of ultralong semiconductor optical amplifiers. After receiving the Ph.D. degree, he was with a patent attorney from 2010 to 2011. Since 2011, he has been with the Fraunhofer Heinrich Hertz Institute (HHI), Berlin, Germany, where he is engaged in the development and fabrication of photodetectors and photonic integrated circuits based on InP. He is currently the Head of the Detector Group, HHI. Since 2020, he has been an Associate Editor for the IEEE JOURNAL OF LIGHTWAVE TECHNOLOGY. Since 2014, he has been a Member of the ECIO steering committee and serves frequently for conference subcommittees, such as CSW-IPRM and OSA APC.

Martin Schell received the Dipl.-Phys. degree from the RWTH Aachen, Aachen, Germany, in 1989, and the Dr. rer. nat. degree from the Technische Universität Berlin, Berlin, Germany, in 1993. He is currently a Professor of optic and optoelectronic integration with the Technical University of Berlin and the Director of the Fraunhofer Heinrich Hertz Institute. He is the Chair of the board of OptecBB (Competence Network Optical Technologies Berlin/Brandenburg), a Member of the Photonics21 board of stakeholders. From 2015 to 2021, he was the Board Member of the European Photonics Industry Consortium. From 2000 to 2005, he was first a product line manager, and then the Head of production and procurement, Infineon Fiber Optics, Munich, Germany. From 1996 to 2000, he was a Management Consultant with the Boston Consulting Group, Boston, MA, USA. Before that, he spent one year as a Visiting Researcher with Tokyo University, Tokyo, Japan.